Extracellular glutathione promotes migration of hydrogen peroxide-stressed cultured chick embryonic skin cells

Mia DeNunzio & George Gomez

In Vitro Cellular & Developmental Biology - Animal

ISSN 1071-2690
Volume 50
Number 4

In Vitro Cell.Dev.Biol.-Animal (2014)
50:350-357
DOI 10.1007/s11626-013-9696-z

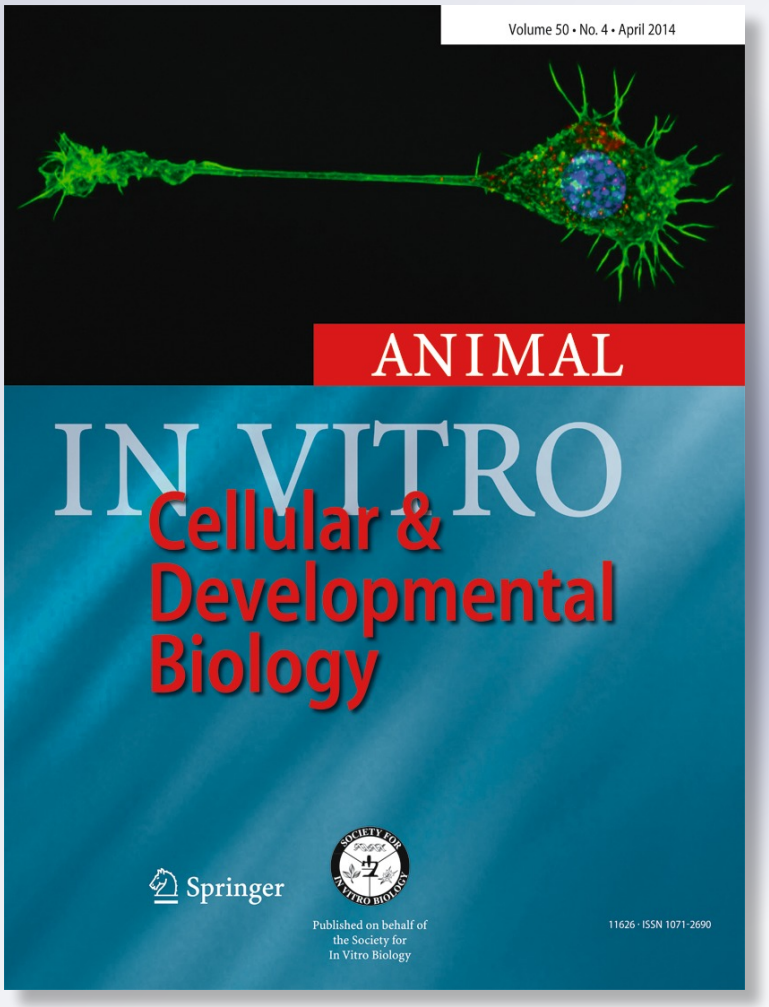

Springer

In Vitro Cell.Dev.Biol.—Animal (2014) 50:350–357
DOI 10.1007/s11626-013-9696-z

Extracellular glutathione promotes migration of hydrogen peroxide-stressed cultured chick embryonic skin cells

Mia DeNunzio · George Gomez

Received: 30 April 2013 / Accepted: 17 September 2013 / Published online: 8 October 2013 / Editor: T. Okamoto

Abstract The ability of glutathione to affect melanocyte survival has fostered its use in a variety of applications related to epithelial cells. Our study focused on fibroblast migration and the effects of oxidative stress. We used scratch assays to measure cell migration: fibroblasts were harvested from embryonic chicks, grown to confluence in a monolayer, and the layer was scratched to initiate migration. Migration rates were measured over 8 h using photomicrographs, and vinculin expression as an indicator focal adhesion formation was measured using immunofluorescence. Addition of 200 μM glutathione to the culture media in which the cells grew resulted in a significantly increased rate of scratch closure. When the scratch assays were performed in the presence of 100 μM H_2O_2 (to simulate oxidative stress), the cells ceased to migrate. Addition of 200 μM glutathione to the H_2O_2-treated scratched layers resulted in a restoration of the scratch closure capabilities. At the subcellular level, addition of extracellular glutathione resulted in a redistribution of vinculin into fewer but larger aggregates. In cells at the edge of scratched monolayers that were treated with H_2O_2, vinculin particles were distributed throughout the cell in smaller aggregates; addition of glutathione resulted in vinculin aggregates that were larger and closer to the edges of the cell, indicating that these cells were more migratory. Our results suggest that glutathione promotes fibroblast migration, possibly via a mechanism that promotes the formation of focal adhesions.

Keywords Epithelial cell migration · Oxidative stress · Glutathione · Antioxidant · Cell adhesion

M. DeNunzio
Biology Department, Fordham University, 113 W. 60th Street, New York, NY 10023, USA

G. Gomez
Biology Department, University of Scranton, 800 Linden Street, Scranton, PA 18510, USA

G. Gomez (✉)
Biology Department, University of Scranton, LSC 395 204 Monroe Ave, Scranton, PA 18510, USA
e-mail: george.gomez@scranton.edu

Introduction

Glutathione (GSH) is a tripeptide found in every mammalian cell that acts in protective pathways against reactive oxygen species such as free radicals. In addition to its known antioxidant function, GSH also plays a variety of alternate roles such as up-regulation of lymphocyte reproduction (for review, see Dröge and Breitkreutz 2000), deoxyribonucleotide synthesis (Holmgren 1979), DNA repair (Lai et al. 1989), regulation of viral synthesis (Kalebic et al. 1991), co-regulators of embryonic development (Takahashi et al. 1993), and inhibitors of melanin synthesis (Yohn et al. 1991, Villarama and Maibach 2005). It is this latter capability that has prompted its use in certain international markets as commercial skin bleaching or whitening products in the form of soaps or cosmetic applications (Gotti et al. 1994; Buschmann and Schollmeyer 2002). While GSH exerts these skin whitening effects due to melanocyte cytotoxicity (Alena et al. 1995), it has also been shown to protect skin fibroblasts against oxidative damage that results from ultraviolet (UV) exposure (Tyrrell and Pidoux 1986). Thus, the spectrum of effects of extracellular GSH on epidermal function has yet to be elucidated. And while the effects of GSH on intracellular proteins and processes are well-studied, few studies focus on the extracellular effects of GSH application (Kopal et al. 2007). Thus, the aim of our research was to focus on the effects extracellular GSH on integumentary processes such as skin cell migration that have implications for other activities such as wound healing.

Embryonic skin is a useful model for the in vivo function of fibroblast cells (Bradley et al. 1980), as these processes utilize similar mechanisms (Martin and Parkhurst 2004). While wound healing involves an interaction between fibroblasts and keratinocytes (Werner et al. 2007), fibroblasts are highly migratory and have been shown to have a faster overall cellular response in comparison to keratinocytes. They are also more susceptible to stress-induced induction and modulation of gene expression (Marionnet et al. 2010), and were thus the focus of this study. To study functional attributes of fibroblasts as reflected in cell migration, we employed a scratch assay technique (Liang et al. 2007) by creating a scratch in a confluent monolayer of cultured fibroblasts and monitored cell migration. Oxidative stress is known to influence fibroblast migration (Mocali et al. 1995). The oxidative stress effects on fibroblasts phenotype and function depend on the level of exposure to reactive oxygen species (Wall et al: 2008); for our study, we used H_2O_2 as the reactive oxygen species at concentrations typically found at wound sites (Schäfer and Werner 2008). Reactive oxygen species can have a myriad of non-specific effects such as protein misfolding (Gregersen and Bross 2010), but can also act through specific mechanisms such as induction of apoptosis that is mediated through activation of the c-Jun N-terminal kinase pathway (Shen and Liu 2006). To measure subcellular effects resulting from treatments with H_2O_2 and extracellular GSH, we focused measuring either actin polymerization into visually distinct filaments (as an indicator of cell migration) or vinculin (as an indicator of focal adhesion formation).

Methods and materials

Tissue harvest and culture. Unless otherwise indicated, materials were obtained from Sigma Chemical Co. (St. Louis, MO).

All equipment and dissecting implements were thoroughly sterilized using 70% ethanol. Chick eggs were obtained from a commercial supplier (CBT Farms, Chestertown, MD). The eggs were incubated in a forced air incubator at 38°C for 14 d. Embryos were removed from the egg and promptly decapitated. Feathers were removed and the skin from the abdomen and chest was stripped from the underlying tissue. The tissue underneath the skin was stripped, minced, and incubated in 0.5% trypsin for 30 min. The tissue was then triturated vigorously for approximately 5 min and then centrifuged for 5 min at 1,000 rpm. The trypsin was decanted and the pellet of cells were resuspended in culture medium (Iscove's Modified Dulbecco's Medium+10% fetal bovine serum+1% penicillin/streptomycin). The cell and culture medium mixture was distributed to sterilized six-well plates containing glass coverslips (22×22 mm, #1 thickness, Thomas Scientific Co, Swedesboro NJ) that were premarked for reference. Cells were grown at 37.0°C, 5.0% CO_2, until a confluent layer of cells had developed (approximately 3–4 d). Under these conditions from this chicken developmental stage, fibroblasts predominate the culture (Rifkin and Crowe 1979; Orkin and Toole 1980).

Scratch assay. An in vitro scratch assay (Liang et al. 2007) was used to assess fibroblast migration. A scratch was made on the confluent layer of cells via a sterile p200 plastic disposable pipette tip (Costar Cat. No. 4864); this made a scratch of approximately 500 μm. For every coverslip, one vertical scratch and two horizontal scratches were made creating two perpendicular intersections along the previously made marks; these intersections served as a visual reference for photomicrographs. The scratches were viewed using an inverted microscope (Nikon TMS) using the 10× objective. A digital camera was used to take photomicrographs of the scratch to document the progress of cell migration every 2 h for 8 h. Two pictures per intersection per coverslip were taken at the exact same places each time interval; this allowed us to observe the same cells migrating to ensure reliable and consistent results. Each picture was taken directly above the intersection of the vertical and horizontal scratches using the point of intersection as a reference. The width of the scratch was measured using the average distance at each point, measured from the farthest edge of each cell along the scratch border. For each coverslip, the width of the scratch at $T=0$ was used as a reference (100%) against which all subsequent measurements were compared.

Cell treatments. The culture medium in each well of the six-well plates was replaced with fresh medium supplemented with GSH (20 or 200 μM) and/or 100 μM H_2O_2; for controls, the medium was replaced with fresh culture medium. Each six-well plate had two coverslips for each treatment condition. Cells were then scratched (as described above) at the specified locations, and photomicrographs were taken ($T=0$). The plates were then returned to the incubator after 5 min at room temperature. At each timepoint ($T=2$ through 8), the plates were taken out and photographed, while ensuring that each plate remained out of the incubator for exactly 5 min.

Immunocytochemistry. Cells were fixed in 4% paraformaldehyde for 10 min. Cells were washed thrice for 5 min in phosphate-buffered saline (PBS), then incubated in blocking solution (PBS+0.3% Triton X+0.1% Normal Goat Serum) for 30 min. Cells were washed thrice in PBS, then incubated overnight in primary antibody (anti-actin, 1:200, mouse monoclonal; anti-vinculin, 1:100,

mouse monoclonal). Cells were then washed three times with PBS and incubated in secondary antibody (goat anti-mouse FITC conjugate 1:200) for 2 h. Nuclei were stained with 4′,6-diamino-2-phenylindole (DAPI) for 5 min. Cells were washed twice with PBS, twice with deionized water, then mounted with Vectashield Hard set (Vector Laboratories, Burlingame, CA) and viewed using an epifluorescence microscope (Nikon TE1000). Epifluorescence images of cells viewed under transmitted and fluorescence illumination were photographed using a digital camera with the exposure set to 500 ms attached to the microscope.

Western blotting. Western blots were conducted using standard immunoblotting techniques. Briefly, tissue was homogenized in 10 mM Tris buffer in the presence of protease inhibitors, and the membrane fraction was purified via high-speed centrifugation. The membrane fraction was separated on a 15% SDS-polyacrylamide gel. Proteins were transferred to a nitrocellulose membrane, incubated for 2 h with 3% of nonfat dry milk, and reacted with anti-vinculin primary antibodies (1:1,000) for 2 h at room temperature. Membranes were washed twice in TBST and incubated for 1 h with peroxidase-conjugated anti-mouse IgG- (1:1,000); antibody staining was visualized with 3,3′-diaminobenzidine for 5–10 min. Uniform gel loading was confirmed using anti-tubulin antibodies (Cell Signaling Technology, Danvers, MA) following manufacturer's instructions.

Data analysis. For all data graphs, values are reported as average±S.E.M. over five full sets of trials. Statistical comparisons were made using the analysis toolpack of Microsoft Excel. The Pearson Correlation was used to compare differences in the rate of scratch closure across different treatments. For all treatments, the significance of the regression lines was >0.95.

Immunostaining images were analyzed using ImageJ (National Institutes of Health, Bethesda MD). For actin staining, the total number of cells and the number with visually distinct polymerized filaments along the scratch edge were noted. For vinculin staining, we focused on 100 individual cells at the edge of the scratch for each treatment condition, and the following measurements were obtained: the total vinculin was computed from the total area (in pixels) covered by the adhesion particles (determined by visual inspection and threshold functions of ImageJ) divided by the total area of the cell (visible from overexposed background fluorescence); the total number of distinct adhesion particles was counted; average particle size was computed by dividing these two measurements. Values for experimental treatments were normalized to the values obtained for the controls (=100%). All particle counts were conducted using the threshold functions and algorithms of ImageJ. Averages were compared using the Students *T* test.

Results

To determine the effects of extracellular GSH in the absence of any stressor, scratch assays were performed on cultured fibroblasts grown in normal media, or in media supplemented with 20 or 200 μM GSH. Upon scratching, cells generally began to migrate into the vacated space, and migrated at a consistent rate to a point where the scratch was approximately 70% of its original width after 8 h (Fig. 1*A*). Addition of 20 μM GSH did not significantly change this rate. Interestingly, 200 μM GSH caused a significant increase in the migration rate of the cells, suggesting that exogenous GSH could augment this normal cellular process.

Fibroblast migration capabilities were greatly hindered by the presence of oxidative stress elicited by H_2O_2, and extracellular GSH rescued the oxidative stress-induced impediment in migration (Fig. 1*B*). Cells exposed to 100 μM H_2O_2 ceased migrating. Our preliminary studies using vital stains to

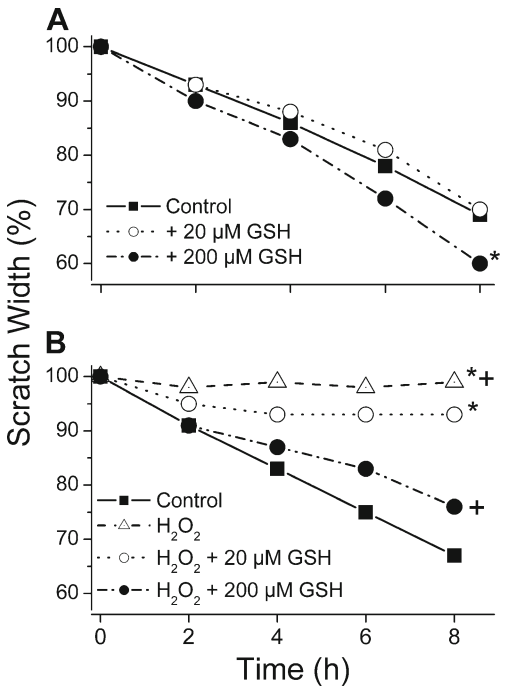

Figure 1. Extracellular glutathione affects overall cell migration. Scratch assays were conducted on cultured skin cells as described in the methods. For this and in subsequent data graphs, each data point presented is an average± S.E.M. over five trials; for clarity, the data points are slightly offset on the *X*-axis. For these graphs, *asterisks* indicate a significant difference from the control, while *plus signs* indicate significant differences of individual treatments from each other. (*A*) To determine the effects of GSH by itself, cells were grown in the presence or absence of GSH (20 or 200 μM). Under control conditions, the progress of scratch closure was relatively consistent over time. Addition of 200 μM GSH resulted in a significantly faster rate of scratch closure. (*B*) Treatment of cells with H_2O_2 resulted in a cessation of cell migration: scratch closure rate was 0. Addition of GSH together with the H_2O_2 resulted in a reduction in the effects of H_2O_2; while 20 μM GSH resulted in a slight but significant increase in closure, 200 μM GSH resulted in a return of the closure rate to one that was not statistically significantly different from the control.

determine cell viability indicated that cells exposed to 100 μM H_2O_2 were still viable within the 8 h time window. The migration was restored by co-addition of 20 μM GSH with 100 μM H_2O_2, although the migration rate was still significantly different slower than in the untreated cells. Addition of 200 μM GSH together with the 100 μM H_2O_2 resulted in a restoration of the migration rate to those found in untreated cells. Thus, the high concentration of GSH helped rescue the cells from oxidative stress-induced migration impediment.

To determine the cellular effects of extracellularly applied GSH, we looked at stress fiber formation (visualized with F-actin immunostaining) and focal adhesion formation (visualized with vinculin immunostaining) in the different treatment conditions. Cells were grown on several coverslips and subjected to scratch assays; a coverslip was removed every 2 h and fixed for immunostaining with actin or vinculin. We focused on measuring immunostaining in cells that were immediately adjacent to the edge of the scratch.

Figure 2 shows sample control cells under immunofluorescence of actin staining (Fig. 2*A*). Some cells had visually distinct actin polymerization typical of stress fibers in migrating cells (Fig. 2*A*), while other cells had depolymerized G-actin typical of quiescent cells (as in Fig. 2*B*). In the untreated (control) cells, nearly all cells immediately adjacent to the edge of the scratch showed actin stress fibers (Fig. 2*A*). When treated with 100 μM H_2O_2 (Fig. 2*B*), cells at the edge of the scratch with polymerized actin were virtually nonexistent; in nearly all cells viewed, the actin was found dispersed throughout the cytosol, with no visually distinct filaments. In the cells treated with 100 μM H_2O_2 and GSH (either 20 μM or 200 μM; Fig. 2*C*, *D*, respectively), cells with actin stress fibers were visible, a clear indication of motile activity. The number of cells lining the edge of the scratch displaying these two types of staining patterns was counted for each treatment; the proportion of cells showing actin polymerization at each timepoint is shown in Fig. 2*E*. There was a significant difference increase in the proportion of cells with visibly distinct filaments in the 20 μM or 200 μM GSH-treated versus control groups of cells exposed to H_2O_2. Interestingly, the proportion of cells showing actin polymerization generally did not increase over the 8 h time period, indicating that either GSH rescued the H_2O_2 effect in only a subset of cells, or that the time window used in our study was too short to see the full-term recovery of the effects.

Vinculin staining was used as a metric of focal adhesion formation and was measured as described above. Our preliminary studies employed a variety of molecules involved with focal adhesions, including integrin, talin, Rac, and paxillin and found that vinculin co-localized perfectly with these various focal adhesion complex molecules. Since vinculin gave us the most reliable and quantifiable staining under our experimental conditions, we used vinculin to measure focal adhesion formation. Figure 4*A* shows a confocal image of vinculin

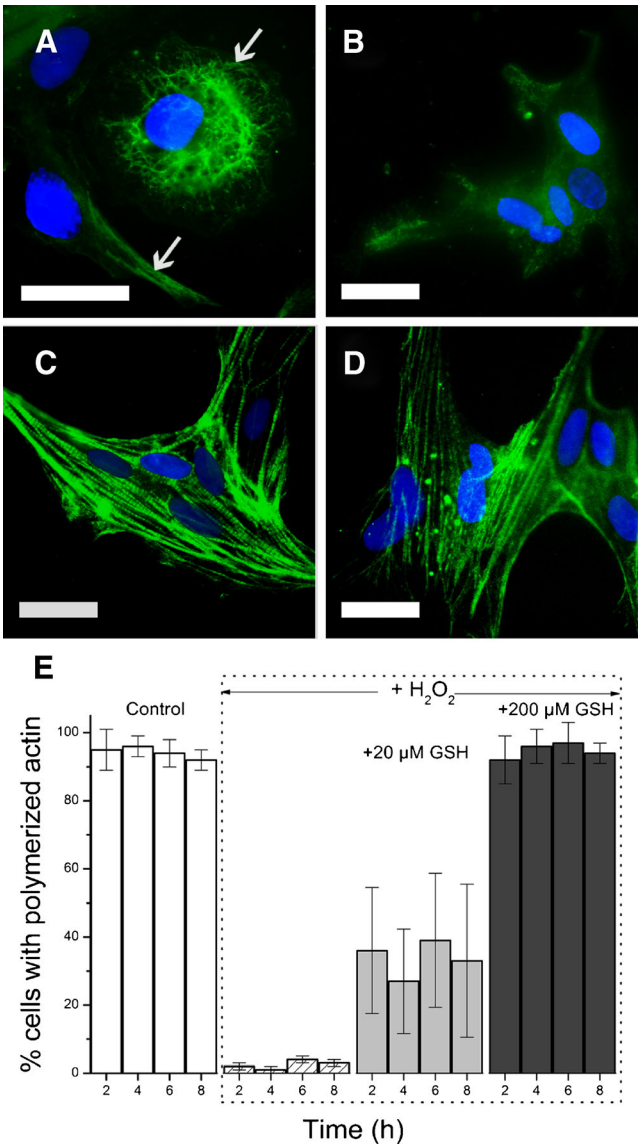

Figure 2. Representative examples of actin polymerization in cells at the edge of a scratch at 2 h. Images are composite photos of epifluorescence of actin (*green*) and nuclei (*blue*); for these images, contrast, and brightness were digitally enhanced to highlight filamentous actin staining. (*A*) Photomicrograph of control cells showing actin immunostaining shows a cell with distinct actin polymerization (*arrows*). (*B*) H_2O_2 treatment resulted in a cessation of cell migration, with no discrete actin polymerization in cells. Addition of 20 μM (*C*) or 200 μM (*D*) glutathione resulted in a greater proportion of visible actin polymerization in cells, with a concomitant increase in cell migration. (*E*) The number of cells displaying along the edge of each scratch displaying discrete actin polymerization was counted. In cells treated with H_2O_2, nearly all cells did not show any actin filament formation or evidence of migratory structures. In controls or in 200 μM GSH+100 μM H_2O_2-treated cells, distinct filaments were visible in nearly all cells that were at the edge of the scratch. In cells treated with 20 μM GSH+100 μM H_2O_2, there was a significant decline in the number of cells that showed actin polymerization; actin staining in these cells was typically dimmer and less pronounced. *Scale bars* for *A*–*D*, 20 μm.

in untreated (control) cells. Addition of 100 μM H_2O_2 radically altered the vinculin expression pattern of the cells on the

scratch edge: the individual focal adhesions were smaller in size and scattered throughout the cell (Fig. 3*B*), a pattern typically seen in non-migrating cells (Mocali et al. 1995). The changes in the H_2O_2-induced vinculin staining pattern were most likely due to redistribution of vinculin rather than changes in overall protein expression. Western blots (Fig. 3*C*) for vinculin in H_2O_2-treated cells at different time points (0–8 h) show no appreciable decrease in intensity of each band, indicating that the total amount of protein did not change over the course of the scratch recovery period. When 20 μM (Fig. 3*D*) or 200 μM GSH (Fig. 3*E*) was added with 100 μM H_2O_2, the vinculin staining pattern resembled that of the control cells: particles were larger, and a large proportion of these were found at the fringes of the cell, a pattern that is typical of healthy, migrating cells (Chen et al. 2000).

To quantify these changes in the adhesion complexes, immunostaining patterns of vinculin particles were measured as described in the methods section. For simplicity, we are showing results from immunostaining at 2 and 8 h post-scratch (Fig. 4). At 2 h, the total amount of vinculin in each cell did not change, but the distribution pattern of the vinculin changed significantly: H_2O_2 caused the vinculin to redistribute into a higher number of small particles, indicating a loss of focal adhesions. Co-addition of GSH with H_2O_2 caused vinculin to aggregate into fewer but larger particles, suggesting the formation of more focused adhesion complexes typical of highly migratory cells (Chen et al. 2000). These distribution patterns were retained after 8 h.

Discussion

Our study examined the effects of extracellularly applied GSH on injury-induced cell migration. Using the in vitro scratch assay, we found that the addition of GSH to the growth medium increased scratch-induced cell migration under normal conditions (Fig. 1*A*), as well as negated the effects of extracellularly applied H_2O_2 on scratch-induced migration (Fig. 1*B*). Our results suggested that GSH influenced the formation of focal adhesion complexes. Integrins that interact with extracellular matrix proteins localize in focal adhesions, and their intracellular domains interact directly with focal adhesion proteins such as vinculin (Burridge et al. 1988). Extracellularly applied GSH resulted in redistribution of vinculin within the peroxide-stressed cells, such that vinculin

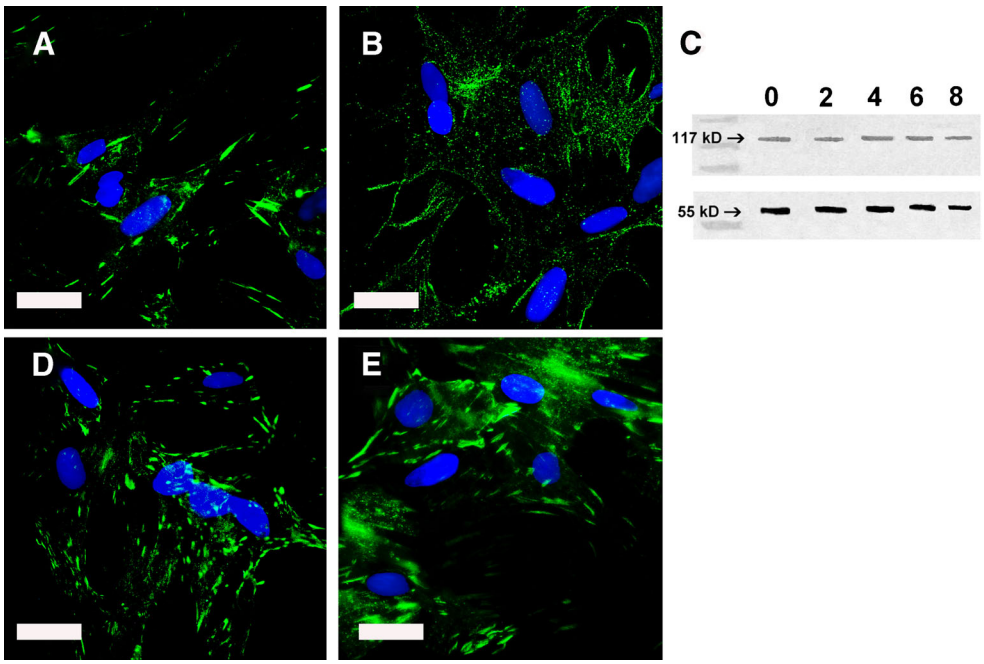

Figure 3. Vinculin staining shows the differences in the formation of cell adhesions in cells found at the edge of the scratch. Images are composite photos of epi-fluorescence of vinculin (*green*) and nuclei (*blue*); for these photos, images were digitally enhanced to highlight vinculin, which appears as *bright discrete dots* or *rods*. (*A*) In control cells, vinculin appeared generally diffuse, with few discrete focal adhesion complexes. (*B*) In H_2O_2-treated cells, vinculin staining was spread throughout the cells, individual particles were generally smaller, and the overall number of vinculin particles was higher. (*C*) Western blots of vinculin from cells treated with H_2O_2 did not show any significant decline in vinculin expression over time, suggesting that the effects of oxidative stress were likely related to protein distribution, and that the GSH rescue was most likely related to mechanisms of protein transport. *Lanes* were loaded as follows: Molecular Weight Standards (bands are at 140 and 110 kDa), and $T=0$ through 8 h post-scratch. The *bottom panel* shows the loading control for the blot, visualized using anti-tubulin antibodies. In cells treated with both H_2O_2 and 20 μM (*D*) or 200 μM GSH (*E*), overall vinculin expression was not greater, but the individual particles were fewer and larger, indicating that the cell was forming more focal adhesions to aid migration. *Scale bars*, 20 μM.

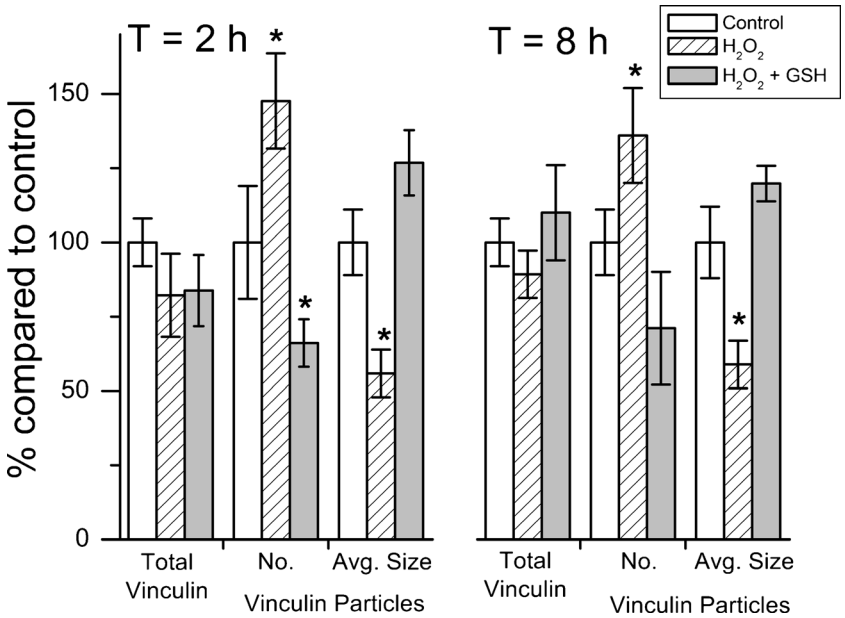

Figure 4. Average vinculin staining patterns for cells found at the edge of the scratch. Cells were treated with 100 μM H_2O_2 with or without 200 μM GSH, or left untreated (*Control*) and scratched. At $T=2$ h and 8 h, cells were fixed and immunostained with vinculin; vinculin expression was measured and analyzed as described in the methods. The number of distinct particles per cell were counted and averaged (*first column*), and the location of each particle (edge of the cell vs. non-edge) was also noted (*second and third columns*). The average amount of vinculin per cell (50 cells were counted for each bar) was measured by counting the average number of pixels per cell in the photographs from the fluorescence images. The average particle size was determined by dividing the values from the fourth column by those in the first column. *Asterisks* denote a significant difference from control.

aggregates were larger and more localized to discrete areas, rather than scattered throughout the cell (Fig. 3), a pattern typically found in migratory fibroblasts (Dunleavy and Couchman 1993).

The wound healing process involves mobilization of both fibroblasts and keratinocytes, which signal each other in a paracrine function to promote differentiation and migration (Werner et al. 2007). During wound healing, mesenchyme-like cells activate early in the process to help lay the matrix upon which keratinocytes migrate; this is the stage in situ that is best represented by our in vitro study. The subsequent reepithelialization driven by keratinocyte migration and proliferation is a key step in wound closure (Gurtner et al. 2008). The act of wounding or scratching is known to trigger the activation of cell signaling pathways that promote wound repair (Steiling et al. 1999; Matsubayashi et al. 2004; Loo et al. 2011). However, it is also thought to trigger production of reactive oxygen species that lead to oxidative stress, which could lead to impediments in cell migration for wound repair (Schäfer and Werner 2008). Thus, in our study, improvements in wound healing due to addition of GSH alone (Fig. 1*A*) possible served as a protective mechanism that acted upon the endogenous oxidants caused by the scratch assay. This is important since stressors such as UVA are known to deplete endogenous glutathione levels in both fibroblasts and keratinocytes, with glutathione depletion being more pronounced in fibroblasts (Niggli and Applegate 1997).

Additional exogenous peroxides that are generated as a result of excessive tissue damage (Schäfer and Werner 2008) or as part of medical wound treatments (O'Toole et al. 1996) present an additional source of oxidant-induced cell damage of both fibroblasts and keratinocytes. Similar to the fibroblasts shown in this study (Fig. 2*A*), non-toxic concentrations of hydrogen peroxide are known to inhibit proliferation and keratinocyte migration on extracellular matrix (O'Toole et al. 1996). Impairments of glutathione metabolism of keratinocytes have shown to be affected by stressors such as organic hydroperoxides (which inactivate GSH peroxidases; Vessey et al. 1992; Vessey and Lee 1993) or UVA (which triggers apoptosis in keratinocytes by inducing GSH efflux; He et al. 2003). In situ, wounding typically results in a depletion of enzyme activity associated with the production of antioxidants (Shukla et al. 1997), making the tissue particularly susceptible to oxidative stress. Such stress results in impaired cellular function, increased apoptosis and necrosis, and reduced migration in cells such as fibroblasts (Colston et al. 2004; Engelmann et al. 2004). Thus, antioxidants such as glutathione could protect these mesenchyme-like cells from stress-induced damage (Kim et al. 2008) resulting in improved fibroblast migration (Fig. 2*A*), increased extracellular matrix deposition, and decreased keratinocyte apoptosis leading to augmented wound healing (Kopal et al. 2007).

Our study did not address the specific mechanism(s) mediating the effect of GSH. Our results suggest that H_2O_2 /GSH

could directly or indirectly interact with cellular mechanisms related to cell adhesion (Fig. 3). However, it is most likely that they were acting through a variety of pathways. In addition to non-specific interactions with sulfhydryl residues on proteins that could lead to changes in their native folded structure (Gregersen and Bross 2010), H_2O_2 is known to interact with cell signaling pathways or molecular switches (for review, see Veal et al. 2007) leading to a variety of cellular effects such as inducing apoptosis, senescent morphogenesis, or altering focal adhesion patterns in fibroblasts (Chen et al. 2000; Shen and Liu 2006). Under H_2O_2-induced stress, GSH most likely acts through its canonical mechanism, where it serves as a proton donor to reactive oxygen species, thus negating the effect of H_2O_2 treatment (Chow and Tappel 1972). However, in the untreated cells, GSH also resulted in an increase in scratch-induced migration (Fig. 1*B*). It is possible that GSH elevated endogenous levels of reactive oxygen species (Kopal et al. 2007) that result from the upregulated cell metabolism that would likely result from injury. However, this does not exclude the possibility that GSH could be acting on alternate mechanisms, such as by interacting with molecules such as Rho GTPases (for review, see Ridley 2001) or Rac (Nobes and Hall 1995), increased activity of matrix metalloproteinases (Kopal et al. 2007), or indirectly through unknown mechanisms. Due to the ubiquitous nature of GSH, it is difficult to ascertain these possibilities, and thus remains an avenue for future investigation.

Our initial motivation for conducting this research was to investigate the use of glutathione in cosmetic products applied to the skin. The results of our research support the possible benefits for the use of glutathione in commercial skin products. Oxidative stress is known to elicit a wide array of destructive effects on cells. In the skin, oxidative stress could result from a variety of exposure to environmental conditions, including UV (Tyrrell and Pidoux 1986). While fibroblasts and keratinocytes possess antioxidant enzymes (with fibroblasts generally possessing more peroxidase, catalase, glutathione peroxidase, and superoxide dismutase activity; Yohn et al. 1991), these could easily be overwhelmed by conditions that generate high levels of oxidative stress (Niggli and Applegate 1997; Loo et al. 2011). The GSH used in these products may offer some minor benefit from increased UV exposure that would inevitably result from skin depigmentation (Alena et al. 1995): the concentration of glutathione in these cosmetic formulations (0.2% by weight) is higher than the concentration used in our study (200 μM), although the actual concentration of GSH that reaches the live skin cell layer is uncertain. While the effects that we studied were limited to wound healing, our results indicate that extracellularly applied GSH could influence intracellular events such as cytoskeletal remodeling and cell adhesion protein expression. This may have implications for the possible beneficial usage of other types of antioxidants in applications related to dermal healing (Kopal et al. 2007; Nevin and Rajamohan 2010).

References

Alena F.; Dixon W.; Thomas P.; Jimbow K. Glutathione plays a key role in the depigmenting and melanocytotoxic action of *N*-acetyl-4-S-cyteaminylphenol in black and yellow hair follicles. *J. Invest. Dermatol.* 104: 792–797; 1995.

Bradley R. A.; Couchman J. R.; Rees D. A. Comparison of the cell cytoskeleton in migratory and stationary chick fibroblasts. *J. Musc. Res. Cell. Motil.* 1: 5–14; 1980.

Burridge K.; Fath K.; Kelly T.; Nuckolls G.; Turner C. Focal adhesions: transmembrane junctions between the extracellular matrix and the cytoskeleton. *Annu. Rev. Cell. Biol.* 4: 487–525; 1988.

Buschmann H. J.; Schollmeyer E. Applications of cyclodextrins in cosmetic products: a review. *J. Cosmet. Sci.* 53: 185–191; 2002.

Chen Q. M.; Tu V. C.; Catania J.; Burton M.; Toussaint O.; Dilley T. Involvement of Rb family proteins, focal adhesion proteins and protein synthesis in senescent morphogenesis induced by hydrogen peroxide. *J. Cell. Sci.* 113: 4087–4098; 2000.

Chow C. K.; Tappel A. L. An enzymatic protective mechanism against lipid peroxidation damage to lungs of ozone-exposed rats. *Lipids* 7: 518–524; 1972.

Colston J. T.; Rosa S. D.; Freeman G. L. Impact of brief oxidant stress on primary adult cardiac fibroblasts. *Biochem. Biophys. Res. Comm.* 316: 258–262; 2004.

Dröge W.; Breitkreutz R. Glutathione and immune function. *Proc. Nutr. Soc.* 59: 595–600; 2000.

Dunleavy J. R.; Couchman J. R. Controlled induction of focal adhesion disassembly and migration in primary fibroblasts. *J. Cell. Sci.* 105: 489–500; 1993.

Engelmann J.; Janke V.; Volk J.; Leyhausen G.; Von Neuhoff N.; Schlegelberger B.; Geurtsen W. Effects of BisGMA on glutathione metabolism and apoptosis inhuman gingival fibroblasts in vitro. *Biomaterials* 25: 4573–4580; 2004.

Gotti R.; Andrisano B.; Cavrini V.; Bongini A. Determination of glutathione in pharmaceuticals and cosmetics by HPLC with UV and fluorescence detection. *Chromatographia* 39: 23–28; 1994.

Gregersen N.; Bross P. Protein misfolding and cellular stress: an overview. *Method Mol. Biol.* 648: 3–23; 2010.

Gurtner G. C.; Werner S.; Barrandon Y.; Longaker M. T. Wound repair and regeneration. *Nature* 453: 314–324; 2008.

He Y.; Huang J.; Ramirez D. C.; Chignell C. F. Role of reduced glutathione efflux in apoptosis of immortalized human keratinocytes induced by UVA. *J. Biol. Chem.* 278: 8058–8064; 2003.

Holmgren A. Glutathione-dependent synthesis of deoxyribonucleotides. Characterization of the enzymatic mechanism of *Escherichia coli* glutaredoxin. *J. Biol. Chem.* 254: 3672–3678; 1979.

Kalebic T.; Kinter A.; Poli G.; Anderson M. E.; Meister A.; Fauci A. S. Suppression of human immunodeficiency virus expression in chronically infected monocytic cells by glutathione, glutathione ester, and *N*-acetylcysteine. *Proc. Natl. Acad. Sci. U.S.A.* 88: 986–990; 1991.

Kim W.-S.; Park B.-S.; Kim H.-K.; Park J.-S.; Kim K.-J.; Choi J.-S.; Chung S.-J.; Kim D.-D.; Sung J.-H. Evidence supporting antioxidant action of adipose-derived stem cells: protection of human dermal fibroblasts from oxidative stress. *J. Dermatol. Sci.* 49: 133–142; 2008.

Kopal C.; Deveci M.; Öztürk S.; Sengezer M. Effects of topical glutathione treatment in rat ischemic wound model. *Ann. Plastic Surg.* 58: 449–455; 2007.

Lai G.; Ozols R. F.; Young R. C.; Hamilton T. C. Effect of glutathione on DNA repair in cisplatin-resistant human ovarian cancer cell lines. *J. Natl. Cancer. Inst.* 81: 535–539; 1989.

Liang C.-C.; Park A. Y.; Guan J.-L. In vitro scratch assay: a convenient and inexpensive method for analysis of cell migration in vitro. *Nat. Protoc.* 2: 329–333; 2007.

Loo A. E. K.; Ho R.; Halliwell B. Mechanism of hydrogen peroxide-induced keratinocyte migration in a scratch-wound model. *Free Rad. Biol. Med.* 51: 884–892; 2011.

Marionnet C.; Pierrard C.; Lejeune F.; Sok J.; Thomas M.; Bernerd F. Different oxidative stress response in keratinocytes and fibroblasts of reconstructed skin exposed to non extreme daily-ultraviolet radiation. *PLoS ONE* 5: e12059; 2010.

Martin P.; Parkhurst S. M. Parallels between tissue repair and embryo morphogenesis. *Development* 131: 3021–3034; 2004.

Matsubayashi Y.; Ebisuya M.; Honjoh S.; Nishida E. ERK activation propagates in epithelial sheets and regulates their migration during wound healing. *Curr. Biol.* 14: 731–735; 2004.

Mocali A.; Caldini C. R.; Chevanne M.; Paoletti F. Induction, effects, and quantification of sublethal oxidative stress by hydrogen peroxide on cultured human fibroblasts. *Exp. Cell. Res.* 216: 388–395; 1995.

Nevin K. G.; Rajamohan T. Effect of topical application of virgin coconut oil on skin components and antioxidant status during dermal wound healing in young rats. *Skin Pharmacol. Physiol.* 23: 290–297; 2010.

Niggli H. J.; Applegate L. A. Glutathione response after UVA irradiation in mitotic and postmitotic human skin fibroblasts and keratinocytes. *Photochem. Photobiol.* 65: 680–684; 1997.

Nobes C. D.; Hall A. Rho, rac, and cdc42 GTPases regulate the assembly of multimolecular focal complexes associated with actin stress fibers, lamellipodia, and filopodia. *Cell* 81: 53–62; 1995.

O'Toole E. A.; Goel M.; Woodley D. T. Hydrogen peroxide inhibits human keratinocyte migration. *Dermatol. Surg* 22: 525–529; 1996.

Orkin R. W.; Toole B. P. Isolation and characterization of hyaluronidase from cultures of chick embryo skin- and muscle-derived fibroblasts. *J. Biol. Chem.* 255: 1036–1042; 1980.

Ridley A. Rho GTPases and cell migration. *J. Cell. Sci.* 114: 2713–2722; 2001.

Rifkin D. B.; Crowe R. M. Tumor promoters induce changes in the chick embryo fibroblast cytoskeleton. *Cell* 18: 361–368; 1979.

Schäfer M.; Werner S. Oxidative stress and normal and impaired wound repair. *Pharmacol. Res.* 58: 165–171; 2008.

Shen H.-M.; Liu Z. JNK signaling pathway is a key modulator in cell death mediated by reactive oxygen and nitrogen species. *Free Radic. Biol. Med* 40: 928–939; 2006.

Shukla A.; Rasik A. M.; Patnaik G. K. Depletion of reduced glutathione, ascorbic acid, vitamin E and antioxidant defence enzymes in a healing cutaneous wound. *Free Radic. Res.* 26: 93–101; 1997.

Steiling H.; Munz B.; Werner S.; Brauchle M. Different types of ROS-scavenging enzymes are expressed during cutaneous wound repair. *Exp. Cell Res.* 247: 484–494; 1999.

Takahashi M.; Nagai T.; Hamano S.; Kuwayama M.; Okamura N.; Okano A. Effect of thiol compounds on in vitro development and intracellular glutathione content of bovine embryos. *Biol. Reprod.* 49: 228–232; 1993.

Tyrrell R. M.; Pidoux M. Endogenous glutathione protects human skin fibroblasts against the cytotoxic action of UVB, UVA and near-visible radiations. *Photochem. Photobiol.* 44: 561–564; 1986.

Veal E. A.; Day A. M.; Morgan B. A. Hydrogen peroxide sensing and signaling. *Molec. Cell* 26: 1–14; 2007.

Vessey D. A.; Lee K. Inactivation of enzymes of the glutathione antioxidant system by treatment of cultured human keratinocytes with peroxides. *J. Invest. Dermatol.* 100: 829–833; 1993.

Vessey D. A.; Lee K.; Blacker K. L. Characterization of the oxidative stress initiated in cultured human keratinocytes by treatment with peroxides. *J. Invest. Dermatol.* 99: 859–863; 1992.

Villarama C. D.; Maibach H. I. Glutathione as a depigmenting agent: an overview. *Int. J. Cosmet. Sci.* 27: 147–153; 2005.

Wall I. B.; Moseley R.; Baird D. M.; Kipling D.; Giles P.; Laffafian I.; Price P. E.; Thomas D. W.; Stephens P. Fibroblast dysfunction is a key factor in the non-healing of chronic venous leg ulcers. *J. Invest. Dermatol.* 128: 2526–2540; 2008.

Werner S.; Krieg T.; Smola H. Keratinocyte–fibroblast interactions in wound healing. *J. Invest. Dermatol.* 127: 998–1008; 2007.

Yohn J. J.; Norris D. A.; Yrastorza D. G.; Bruno I. J.; Leff J. A.; Hake S. S.; Repine J. E. Disparate antioxidant enzyme activities in cultured human cutaneous fibroblasts, keratinocytes, and melanocytes. *J. Invest. Dermatol.* 97: 405–409; 1991.